Environ Fluid Mech (2007) 7:95–119
DOI 10.1007/s10652-007-9018-7

ORIGINAL ARTICLE

The impact on tropospheric ozone formation on the implementation of a program for mobile emissions control: a case study in São Paulo, Brazil

Odón R. Sánchez-Ccoyllo · Leila Droprinchinski Martins · Rita Y. Ynoue · Maria de Fátima Andrade

Received: 27 September 2005 / Accepted: 15 January 2007 / Published online: 2 March 2007
© Springer Science+Business Media B.V. 2007

Abstract The main sources of reactive hydrocarbons (RHC) and nitrogen oxides (NO_x), ozone precursors, in the Metropolitan Area of São Paulo (MASP) in the southeast of Brazil are emissions from vehicles fleets. Ambient surface ozone and particulate matter concentrations are air quality problem in the MASP. This study examined the impact that implementing a control program for mobile emissions has on ozone concentrations, An episode of high surface ozone concentrations occurring in the MASP during the March 13–15, 2000 period was used as a case study that was modeled for photochemical oxidants using the California Institute of Technology/Carnegie Mellon University three-dimensional photochemical model. Different scenarios were analyzed in relationship to the implementation of the *Programa Nacional de Controle de Poluição por Veículos Automotores* (PROCONVE, National Program to Control Motor Vehicle Pollution). Scenario 1 assumed that all vehicles were operating within PROCONVE guidelines. Scenarios 2 and 3 considered hypothetical situations in which the PROCONVE was not implemented. Scenario 2 set the premise that vehicles were using pre-1989 technology, whereas scenario 3 allowed for technological advances. A base case scenario, in which the official emission inventory for the year 2000 was employed, was also analyzed. The CIT model results show agreement with most measurements collected during 13–15 March 2000 modeling episode. Mean normalized bias for ozone, CO, RHC and NO_x are approximately 9.0, 6.0, −8.3, 13.0%, respectively. Tropospheric ozone concentrations predicted for scenario 2 were higher than those predicted for scenarios 1, 3 and base case. This study makes a significant contribution to the evaluation of air quality improvement and provides data for use in evaluating the economic costs of implementing a program of motor vehicle pollution control aimed at protecting human health.

O. R. Sánchez-Ccoyllo (✉) · L. D. Martins · R. Y. Ynoue · M. F. Andrade
Department of Atmospheric Sciences at the Institute of Astronomy, Geophysics and Atmospheric Sciences, University of São Paulo, Rua do Matão, 1226-Cidade Universitária, São Paulo, SP 05508-090, Brazil
e-mail: osanchez@model.iag.usp.br

Keywords Air quality · CIT model · Emission inventory · Ozone · São Paulo

Abbreviations

CETESB	*Companhia de Tecnologia de Saneamento Ambiental* (Environmental Sanitation Technology Company)
CIT model	Photochemical Model developed jointly by Carnegie Mellon University and the California Institute of Technology
IAG	Institute of Astronomy, Geophysics and Atmospheric Sciences
MASP	Metropolitan Area of São Paulo
NO_x	Oxides of nitrogen
ppbv	Parts per billion by volume
PROCONVE	*Programa Nacional de Controle de Poluição por Veículos Automotores* (National Program to Control Motor Vehicle Pollution)
RAMS	Regional atmospheric modeling system
SAPRC	Statewide Air Pollution Research Center
SODAR	Sound detection and ranging
USP	University of São Paulo
VOC	Volatile organic compound
RHC	Reactive hydrocarbons

1 Introduction

Elevated surface ozone and particulate matter concentrations are a persistent pollution problem in the metropolitan area of São Paulo (MASP). In the MASP, ozone levels routinely exceed the 1-hour standard (82 ppbv) and the attention (102 ppbv) established by the Brazilian National Ambient Air Quality Monitoring Program. Ozone control is problematic since tropospheric ozone production is the result of a complex set of photochemical reactions and precursor emissions inventories [1]. The assessment of an ozone strategy is a difficult task, requiring the application of a suitable photochemical model. Such a model must have a comprehensive chemical mechanism in order to describe the relationships among the various classes of volatile organic compounds (VOCs) and oxides of nitrogen (NO_x). Photochemical air quality models are useful tools that can predict the non-linear response of pollutant concentrations to changes in precursor emission rates. Confidence is established in the ability of an air quality model to predict existing pollutant trends during a representative air quality episode [2]. Air pollutant emissions inventories are constructed using two different approaches: *top-down and bottom-up* [3]. The top-down approach seeks to validate the emission inventory by making independent estimates of emissions, such as that achieved by examining the compatibility between emission inventory-based emission estimates and air quality measurements. The bottom-up approach relies in detailed emission models and methodologies for estimating emissions factors. When top-down and bottom-up estimates agree well, emission inventories can be considered more reliable. The urban emissions inventory for the MASP was compiled, using bottom-up approach, by the *Companhia de Tecnologia de Saneamento Ambiental* (CETESB, Environmental Sanitation Technology Company) of the state of São Paulo.

Table 1 Emissions inventory scenario for the year 2000 with PROCONVE constraints

	CO	HC	NO_x	SO_2
Gasoline vapor	0.0	13.6	0.0	0.0
Gasoline liquid	0.0	146	0.0	0.0
Gasoline exhaust	754.0	78.8	33.5	13.1
Alcohol vapor	0.0	1.4	0.0	0.0
Alcohol liquid	0.0	18.3	0.0	0.0
Alcohol exhaust	345.3	38.5	18.2	0.0
Diesel vapor	0.0	0.0	0.0	0.0
Diesel liquid	0.0	0.0	0.0	0.0
Diesel exhaust	401.0	65.3	293.0	25.5
Total	1500.3	361.9	344.7	38.6

Values expressed as 1000 ton $year^{-1}$ units; CO, carbon monoxide; HC, hydrocarbons; NO_x, oxides of nitrogen; SO_2, sulfur dioxide; ton, weight of 1000 kg

Table 2 Emission standards for new cars in Brazil (g km^{-1})

Year	Carbon monoxide	Hydrocarbons	Oxides of nitrogen
1988	24.0	2.1	2.0
1992	12.0	1.2	1.4
1997	2.0	0.3	0.6
2005	2.0	0.16	0.25
2009	2.0	0.05	0.12

Sources: *Conselho Nacional do Meio Ambiente* (CONAMA, Brazilian national environmental code) resolution number 18, 1986; the *Instituto Brasileiro do Meio Ambiente e dos Recursos Naturais Renováveis* (IBAMA, Brazilian Institute for Environment and Renewable Natural Resources) – http://www.ibama.gov.br

In the present study, the CETESB emissions inventories, as well as emissions scenarios based on a report by La Rovere et al. [4], were taken into consideration, during a typical pollution episode. Three different scenarios were considered. In scenario 1 (Table 1), all vehicles are in compliance with the standards set by the *Programa Nacional de Controle de Poluição por Veículos Automotores* (PROCONVE, National Program to Control Motor Vehicle Pollution). The PROCONVE is a Brazilian program aimed at controlling pollutant emissions from mobile sources. The program sets targets for new vehicle emission controls, according to the timetable presented in Table 2. Scenario 2 is based on the premise that the PROCONVE does not exist, and that vehicles are using pre-1989 technology (Table 3). Scenario 3 also assumes that there is no PROCONVE but allows for progressive technological evolution of vehicle design (Table 4). These scenarios were compared to the base case scenario, in which the CETESB emissions inventory for the year 2000 was used (Table 5). Data interpolation routine included in CIT model, which was developed jointly by Carnegie Mellon University and the California Institute of Technology [5], was employed in constructing the meteorological fields since the air chemistry diagnostic portion of the CIT model is more dependent on the input observed data. Observed wind fields were obtained from: CETESB monitoring stations; the climatological station of the University of São Paulo (USP) Institute of Astronomy, Geophysics and Atmospheric Sciences (IAG); Doppler Sound Detection And Ranging (SODAR) data. In addition, simulated wind fields have been obtained from Regional Atmospheric

Table 3 Emissions inventory scenario for the year 2000 without PROCONVE constraints and with pre-1989 technology

	CO	HC	NO_x	SO_2
Gasoline vapor	0.0	13.6	0.0	0.0
Gasoline liquid	0.0	146.0	0.0	0.0
Gasoline exhaust	1977.0	190.6	63.5	13.1
Alcohol vapor	0.0	1.4	0.0	0.0
Alcohol liquid	0.0	18.3	0.0	0.0
Alcohol exhaust	380.5	41.4	19.6	0.0
Diesel vapor	0.0	0.0	0.0	0.0
Diesel liquid	0.0	0.0	0.0	0.0
Diesel exhaust	401.0	65.3	293.0	25.5
Total	2758.5	476.6	376.1	38.6

Values expressed as 1000 ton $year^{-1}$ units; CO, carbon monoxide; HC, hydrocarbons; NO_x, oxides of nitrogen; SO_2, sulfur dioxide; ton, weight of 1000 kg

Table 4 Emissions inventory scenario for the year 2000 without PROCONVE constraints and allowing for technological evolution

	CO	HC	NO_x	SO_2
Gasoline vapor	0.0	13.6	0.0	0.0
Gasoline liquid	0.0	146.0	0.0	0.0
Gasoline exhaust	953.6	99.1	47.1	13.1
Alcohol vapor	0.0	1.4	0.0	0.0
Alcohol liquid	0.0	18.3	0.0	0.0
Alcohol exhaust	352.6	39.3	18.6	0.0
Diesel vapor	0.0	0.0	0.0	0.0
Diesel liquid	0.0	0.0	0.0	0.0
Diesel exhaust	401.0	65.3	293.0	25.5
Total	1707.2	383.0	358.7	38.6

Values expressed as 1000 ton $year^{-1}$ units; CO, carbon monoxide; HC, hydrocarbons; NO_x, oxides of nitrogen; SO_2, sulfur dioxide; ton, weight of 1000 kg

Modeling System (RAMS) meteorological model output [6,7], where (outside of the MASP area) observed surface meteorological variables do not exist. RAMS output was inserted as "virtual stations".

The CIT Eulerian airshed model [5,8] was applied to simulate the photochemical events of March 13–15, 2000 in the MASP. The CIT model, using an air emissions inventory and meteorological data, simulates the fate and transport of photochemical pollutants in the atmosphere [9]. In the MASP, there are several studies analyzing the photochemical air pollution using CIT airshed model. For example, Sánchez-Ccoyllo et al. [10] performed the local sensitivity analysis of CIT model in the MASP, i.e., they solved the system repeatedly while varying one parameter at a time and fixing the other variables. They found that changes in mixing height, wind speed and air temperature input files have the greatest effect on peak ozone in the MASP, and the isolated effect of RHC emission inventory reduction leads to 26% lower ozone levels than in the base case. Vivanco and Andrade [11] investigated inaccuracies in the mobile emissions data. They found that NO_x and RHC CETESB'S official emission inventory by motor vehicles are respectively overestimated and slightly underestimated. Ulke and Andrade [12] introduced an alternative vertical turbulence parameterization in

Table 5 Official motor vehicles and stationary emissions inventory scenario from CETESB for the year 2000. Base case scenario

	CO	HC	NO_x	SO_2
Gasoline vapor	0.0	14.2	0.0	0.0
Gasoline liquid	0.0	134.7	0.0	0.0
Gasoline exhaust	996.5	105.6	50.3	10.8
Acohol vapor	0.0	1.0	0.0	0.0
Alcohol liquid	0.0	17.7	0.0	0.0
Alcohol exhaust	209.5	23.5	13.0	0.0
Diesel vapor	0.0	0.0	0.0	0.0
Diesel liquid	0.0	0.0	0.0	0.0
Diesel exhaust	417.2	68.0	304.7	10.4
Total mobile vehicles	1623.2	364.7	368.0	21.2
Stationary source(number of inventory industries)	38.6 (750)	12.0 (800)	14.0 (740)	17.1 (245)
Total vehicle + stationary	1661.8	376.7	382.0	38.3
% of mobile vehicles	97.7	96.8	96.3	55.4
% of stationary source	2.3	3.2	3.7	44.6

Values expressed as 1000 ton $year^{-1}$ units; CO, carbon monoxide; HC, hydrocarbons; NO_x, oxides of nitrogen; SO_2, sulfur dioxide; ton, weight of 1000 kg

the CIT model and analyzed the impact on the behavior of air pollutants. They found that the application of the proposed parameterization lead to increased predicted concentrations. The MASP, which comprises the city of São Paulo (23°33′S, 46°45′W) and its 38 neighboring municipal districts (cities), it covers an 8,000 km^2 area, with a population of 18 million people and a light-duty fleet of 7.4 million vehicles [13]. Local weather is often strongly affected by circulations induced as a result of the influence of the complex terrain and large water reservoirs. On summer days dominated by the Atlantic subtropical high pressure zone, two phenomena are observed in the MASP: afternoon storms and nocturnal fog. The city of São Paulo City is located on a plateau approximately 50 km from the ocean. Two mountain ranges, the Cantareira Ridge (at the edge of the plateau) and the Serra do Mar, lie between the MASP and the Atlantic [14].

2 Modeling methods

2.1 Formulation of the CIT airshed model

The CIT airshed model is a three-dimensional Eulerian photochemical model based on a numerical solution of the atmospheric diffusion equation. The CIT model describes the formation and transport of chemically reactive pollutants in the turbulent planetary boundary layer [5,8].

This three-dimensional model solves the atmospheric dispersion equations with chemical reaction [5,15]:

$$\frac{\partial C_i}{\partial t} + \nabla \cdot (uC_i) = \nabla \cdot (K \nabla C_i) + R_i(C_i, \ldots, C_p) \quad (1)$$

Subject to initial and boundary conditions, data on the meteorological conditions, and the emissions of ozone precursors.

$$C_i(x\partial\Omega, y\partial\Omega, t) = C_i\partial\Omega, \tag{2}$$

$$\frac{\partial C_i(z=0,t)}{\partial z} = S_i + v_g C_i, \tag{3}$$

$$\frac{\partial C_i(z=H,t)}{\partial z} = 0, \tag{4}$$

$$C_i(x,y,z,0) = C_{i0}, \tag{5}$$

where $C_i, x, z, t, u, K, R_i, S_i, v_g, H$ and $\partial\Omega$ are, respectively, the concentration of species i, space variables, time variable, wind fields, diffusion fields, chemical kinetics, source, settling velocity, inversion height and domain boundary.

An inevitable consequence of using CIT model to describe complex system is that some approximations are involved. These uncertainties arise either from the characterization of the physical processes or from the measurement errors inherent in CIT model input variables. The goal of any sensitivity analysis is to determine the form of the system output resulting from the parameters variations; it is called local sensitivity analysis. An analysis which accounts for simultaneous variations in all the parameters over their full range of uncertainties is called a global method [16].

Sensitivity analyses of the Eqs. 1–5 have been made by studying individual elements of the basic model. For example, Falls et al. [17] investigated the influence of parameter variations on the predictions of a photochemical reactions mechanism. They showed that the major sensitivity of the NO_2, O_3, and PAN concentrations lies in photolysis rates for NO_2 and aldehydes. On the other hand, for the global analysis(sensitivity/uncertainty), generalized stoichiometric coefficients and certain rate constants have had shown to exert the most influence on the predictions of the mechanism. Koda et al. [18] used the Fourier Amplitude Sensitivity Test (FAST) method to examine the effects on uncertainties in specification of the vertical turbulent transport. The principal finding from their study was that the concentrations predictions were most sensitive to variations of the turbulent diffusivity, K(z), close to the surface.

Seefeld and Stockwell [19] investigated the relative importance of reactions that affect ozone and PAN concentrations with the Regional Atmospheric Chemistry Mechanism. They showed that even thought ozone concentrations may be very similar between a case with constant photolysis and a case with diurnally varying photolysis rates, that the processes affecting the ozone concentrations may be quite different. Daescu et al. [20] presented an extensive set of numerical experiments and applications of the new Kinetic Pre-Processor (KPP) to direct decoupled and adjoint sensitivity analysis. Their results indicated that KPP may be used as a flexible and efficient tool to generate code for sensitivity studies of the chemical reactions mechanism. Kioutsioukis et al. [21] studied the sensitivity analysis of the model emission estimates, using Extended FAST, a technique based on the decomposition of the output variance. They found that: (i) uncertainty in NO_x emissions is the main source of the uncertainties of the emission factors; and (ii) uncertainty in RHC and particulate

matter emissions depends mainly upon the diesel share between passenger cars and LDVs, by emission factors and by the average trip length.

In order to compute spatially averaged hourly values of atmospheric concentrations of multiple gaseous air pollutants, the CIT model requires that land use and emissions inventory be defined over the modeling grid, and that wind, temperature, humidity, solar radiation and atmospheric boundary layer depth information be included.

For model input, a divergence-free, three-dimensional wind-field is constructed, and this, together with all other raw data, is stored at 1 h intervals in two- or three-dimensional grids as appropriate [5,22]. In the MASP, the CIT model equations are solved using the method of operator splitting [8]. Operator splitting methods [23] are employed in the CIT model to reduce the computational effort required to solve the governing equations. In each time-step, x-advection/diffusion is followed by y-advection/diffusion. The vertical advection/diffusion is achieved through combined integration of reaction and emissions input. The advection scheme employs a finite-element Galerkin method and subsequent non-linear filtering [5,22].

The CIT model is structured such that the advection/diffusion solution for the chemical species proceed in parallel, and, for the calculation of reaction rates, concentrations are exchanged only once per time-step [5,22]. The chemical mechanism in the CIT model represents the processes by which primary pollutants, such as VOCs and NO_x, interact in the gas phase to form secondary pollutants such as ozone and other oxidants. This is an important component of airshed models because if the mechanism is incorrect or incomplete in significant respects, then the model's predictions of secondary pollutant formation may also be incorrect, and its use might result in implementation of inappropriate or even counter-productive air pollution control strategies [24,25]. The latest version of the Statewide Air Pollution Research Center (SAPRC) chemical mechanism, the SAPRC-99, developed by the SAPRC at the University of California [25], was used in this study. In addition, the SAPRC-99 is a completely updated and expanded version, superseding all previous SAPRCs [26–28]. The major components of the SAPRC mechanisms are: (i) the base mechanism, (ii) the assignments and/or estimation procedures used to estimate the reactions of the represented VOCs that are not in the base mechanism, and (iii) the lumping procedures used to represent complex mixtures or VOCs for which assignments or estimates are not available. The base mechanism is the portion of the mechanism that represents the reactions of the inorganic species, the common organic products, the intermediate radicals leading to these products, including those formed from the initial reactions of the represented VOCs not in the base mechanism.

Airshed model applications require simulations of highly complex mixtures of large numbers of VOCs. For such applications, models with lumped model species that represent reactions of a large number of species with similar reaction rates and mechanisms, are employed. The SAPRC-99 mechanism, two different approaches, referred to as lumped molecule and variable lumped parameter condensation, can be employed to represent VOCs in complex mixtures using this mechanism. The lumped molecule approach involves representing the VOC by a model species in the base mechanism, on a molecule-for-molecule basis. The variable lumped parameter approach representing a group of VOCs that react with similar rate constants with model species whose kinetic and product yield parameters are weighted averages of the mixture of VOCs they are being used to represent [25]. This mechanism has assignments for 400 types of VOCs and can be used to estimate reactivities for 550 VOC categories. The inorganic reactions in the mechanism are essentially the same

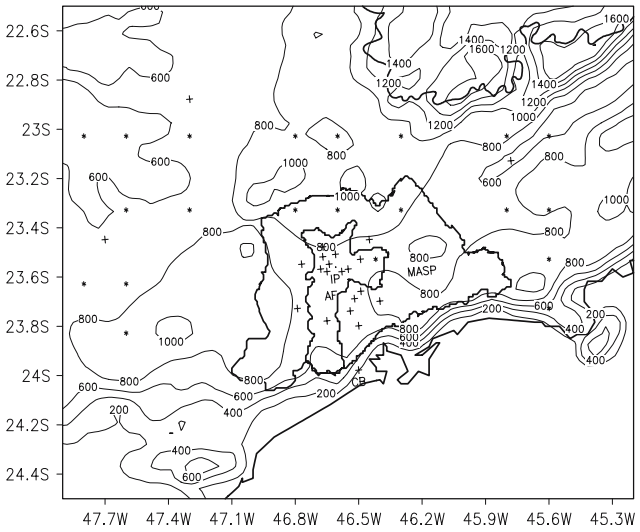

Fig. 1 Modeling domain and distribution of monitoring CETESB air quality stations (+) and meteorological virtual stations (*) that generated by meteorological model named RAMS. AF is a climatological station operated by University of Sao Paulo. IP and CB over map are Ibirapuera Park and Cubatao Centro where performed SODAR measured. Topography: altitude in meters

as those included in the previous version [25]. The species used in the base mechanism and lumped mechanism, their reactions and constants, the rate constant, and the absorption cross section and quantum yields for the photolysis reaction are described by Carter [25]. The major differences between this SAPRC-99 and all previous SAPRC mechanism [26–28] include the following: updated rates constants, absorption cross sections, quantum yields, and reaction mechanisms; the base mechanism was modified to improve somewhat the accuracy and level of detail in the mechanism in representing no-NOx or low-NOx conditions. The methyl peroxy and acetyl peroxy radical model species are represented explicitly; The PAN analogue formed from glyoxal is lumped with the rest of the higher PAN analogues. Isoprene photooxidation products are included; Reactions of O^3P with O_3 and NO were included; the reaction of OH with HONO was included;

In the present study, the SAPRC-99 mechanism used in the CIT model consisted of 70 species in 223 reactions. The species include 4 constant species, 14 stable inorganic species, 6 inorganic short-lived species, 24 stable organic species, 14 organic short-lived species, 4 peroxyacetyl nitrates and analogues and 4 stable aromatic species, as described by Carter [25].

2.2 Target domain and period

Figure 1 shows the 300 × 150 km study area centered in the MASP. The domain is horizontally divided into a $5 \times 5\,km^2$ regular grid such as that described by Kuebler et al. [15]. Vertically, there are five layers up to the model top at 2100 m. The CIT photochemical airshed model uses a terrain-following coordinate system that transforms

Table 6 Number station of CETESB air quality station (NE), site code, description, and coordinates in the Sao Paulo Metropolitan Area. Grid cell refers to the computational coordinate system

NE[a]	Code	Site description	Coordinate (km)		Grid cell		Elevation (m)
			X	Y	X	Y	
04	CAMB	Cambuci	335.5	7392.7	27.1	14.5	740
42	CAMP	Campinas	289.0	7465.8	17.8	29.2	650
10	CCES	Cerqueira Cesar	329.4	7395.1	25.9	15.0	780
12	CENT	Centro	332.3	7395.1	26.5	15.0	730
08	CONG	Congonhas	330.6	7388.2	26.1	13.6	760
24	CBCT	Cubatao - Centro	355.8	7358.3	31.2	7.7	7
25	CBVP	Cubatao - Vila Parisi	359.2	7362.5	31.8	8.5	10
15	DIAD	Diadema	335.5	7381.0	27.1	12.2	800
13	GUAR	Guarulhos	347.6	7404.9	29.5	17.0	750
05	IBIR	Ibirapuera	330.9	7391.1	26.2	14.2	750
09	LAPA	Lapa	327.0	7398.9	25.4	15.8	720
22	MAUA	Mauá	351.0	7382.9	30.2	12.6	760
03	MOOC	Mooca	336.7	7395.0	27.3	15.0	740
17	OSAS	Osasco	318.8	7396.9	23.8	15.4	720
01	PQDP	Parque D. Pedro	333.7	7395.2	26.7	15.0	730
11	PENH	Penha	345.1	7397.7	29.0	15.5	700
27	PINH	Pinheiros	326.3	7393.3	25.3	14.7	720
16	SAMO	Santo Amaro	326.0	7383.2	25.2	12.6	730
18	SACP	Santo Andre – Capuava	347.8	7384.9	29.6	13.0	800
14	SACT	Santo Andre – Centro	343.3	7384.6	28.7	12.9	760
02	SANT	Santana	333.0	7394.9	26.6	15.0	730
19	SBCP	São Bernardo do Campo	337.7	7384.0	27.5	12.8	740
07	SCSU	Sao Caetano do Sul	339.6	7388.9	27.9	13.8	740
21	SMPT	Sao Miguel Paulista	351.1	7400.3	30.2	16.1	800
55	SJCA	Sao Jose Dos Campos	410.9	7435.5	42.2	23.1	600
51	SORO	Sorocaba	246.9	7398.7	9.4	15.7	650
20	TBSE	Taboao da Serra	321.0	7379.5	24.2	11.9	780
	IAGU	Agua Funda	334.5	7383.4	26.9	12.7	760

[a] Number station of CETESB air quality station in the Sao Paulo metropolitan area

physical domain grid points, into a more convenient computational domain [2,5]. The vertical layers are logarithmically spaced [2], with thicknesses of 73 m (at the lowest level), 223, 294, 693, and 819 m, yielding a total column depth of 2100 m. in addition, also, Fig. 1 also shows the locations of CETESB air quality stations, virtual stations for surface meteorological data, and location of SODAR measured (upper level meteorological data), and the topography that was obtained from the United States Geological Survey (USGS) topography dataset [30]. It is defined as 30 arc-second (approximately 1-km) latitude–longitude [31]. The CETESB monitoring stations data used to provide the initial and boundary conditions as well to validate the model are presented in Table 6 regarding the sampling site coordinates. Figure 2 presents the diurnal variation in ozone concentrations observed at CETESB monitoring stations, localized in the MASP and available for the modeling period: PQDP, IBIR, OSAS, PINH, MOOC and SANT [32,33]. Ozone concentrations were elevated, especially at the IBIR station. The directive's long-term objective to protect human health (maximum ozone concentration of 120 μg m^{-3} over 8 h) was extensively exceeded in the region during period, mainly on March 16.

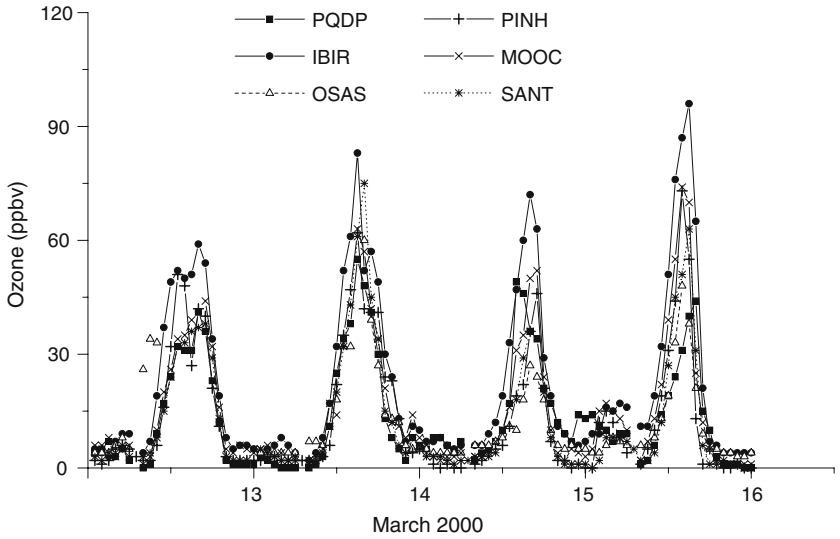

Fig. 2 Variation in surface ozone concentrations (ppbv) at the air quality monitoring stations in the MASP – March 13–16, 2000. PQDP, Parque Dom Pedro; IBIR, Ibirapuera Park; OSAS, Oasco; PINH, Pinheiros; MOOC, Mooca; SANT, Santana

2.3 Meteorological data

Monitoring stations were mostly confined to the MASP. Surface monitoring stations include 28 CETESB monitoring stations and the IAG-USP climatological station. Since the modeled area is larger than MASP, meteorological data where there were no observations was obtained by "virtual stations", as shown in Fig. 1. Wind field was then obtained by interpolation procedures using both real and virtual stations to a regular grid using inverse distance-squared weighting [34]. Following the interpolation procedure, a local terrain adjustment technique, involving solution of the Poison equation, is used to establish the horizontal component of the surface field. To interpolation of the upper level wind data is used a Doppler SODAR measurement data from two CETESB stations: IBIR and CBCT (Fig. 1). The SODAR has been reported in detail by Nair et al. [35]. The approach taken for spatial interpolation of upper level wind data is r^{-1} weighting. The final step is to generate vertical velocities (w) from successive solution of the continuity equation followed by an interactive procedure, which reduces anomalous divergence in the complete field [34].

The mixing heights are derived from the Doppler SODAR data from two CETESB stations: Ibirapuera Park and Cubatao Centro. During the modeling period, the mixing heights at 1500 local time (LT) were 1020–1870 m, whereas those at 0300 LT were 340–850 m. Spatial and temporal variations in mixing heights were obtained by interpolating the mixing heights measured at IBIR and CBCT using the r^{-1} procedure.

Other surface meteorological variables, such as temperature and humidity, were interpolated using the Barnes scheme [36].

The CIT airshed model has a set of default levels of the actinic irradiance that are obtained from a function of zenith angle that assumes a cloud free sky [37, 38]. Photolysis rates were calculated using Peterson's actinic flux estimates [39]. So,

for ultraviolet solar radiation during the modeled period, clear sky conditions were assumed.

In this study, virtual stations derived from the prognostic Mesoscale RAMS (RAMS 4.3) provided the meteorological data for input into the CIT model [40,41]. Land use, land cover and surface roughness heights data for each computational cell have been developed to extract from meteorological model RAMS. Surface resistances for gaseous pollutants for these computational cell were estimated based on the cell's land use and land cover types using the method described by Russell et al. [42].

2.4 Emission data

The distributions of NO_x, CO, RHC and SO_2 emissions throughout the MASP were taken into consideration. Table 5 depicts the base case scenario for 2000, the data from which were used as emission profile input for the CIT model. In this Table 5, these data are shown of mobile and stationary sources in the emission of ozone precursors. According to Andrade et al. [32] it is very difficult to accurately resolve stationary elevated sources because this information is not made available to the public. According these data from CETESB (Table 5), 2.3, 3.2, and 3.7% of CO, RHC, and NO_x in the MASP are emission originate from stationary sources, however, 97.7, 96.8, and 96.3% of CO, RHC, and NO_x are from vehicular emission. This agreement with Andrade et al. [32] and Alonso et al. [43] that stationary sources have a very small impact on the emission of gases to the atmosphere in the MASP. Electric power in the MASP is generated almost solely by hydroelectric power stations. In the 1980s, many factories converted from boilers to electrical energy sources.

All mobile and point sources were combined on a $5 \times 5\,km^2$ grid base. Below describes the procedures used to allocate emissions into the appropriate computational cells [5]. Point source, needs to be treated as direct inputs to the atmosphere diffusion equation (Eq. 1 in item 2 above).

The spatial distribution of mobile vehicles emissions was calculated a proportional to the number of registered vehicles in each city of 39 municipalities belonging to the MASP area (Fig. 3). These data regarding the number vehicles were obtained from DETRAN [44]. In addition to mobile emissions in the MASP, mobile emissions from the cities of SJCA, Baixada Santista and SORO were added. In 2000 year, the MASP were approximately 6.9 million passenger and commercial vehicles: 93.5% light-duty vehicles (LDVs) and 6.5% heavy-duty diesel vehicles (HDVs). Of the LDVs, approximately 76.3% burn a mixture of 78–80% (v/v) gasoline and 22% ethanol (refered to as gasohol), and 17.2% use hydrated ethanol (95% ethanol +5% water). Only the São Paulo city represented for approximately 76% of the vehicles to hydrated ethanol and the gasohol and 70% of the HDVs, so, all CO, RHC, NO_x and SO_2 mobile emissions are high in São Paulo city with 49 points of grid cell.

The temporal distribution of mobile emissions for each day was based on tunnel measurements. These measurements were performed in two road tunnels in the MASP, namely Janio Quadros (JQ) and Maria Maluf (MM), on March and May 2004, respectively. JQ tunnel carried mainly LDVs, whereas MM tunnel carried both LDVs and HDVs. These experiments are described in more detail by Martins et al. [45] and Sánchez-Ccoyllo et al. [46]. Then, for temporal distribution of LDVs (two peaks during the day for LDVs at 0800, 0900 local time-LT and 1800, 1900 LT, see Fig. 4), it used the emission factors (EFs) estimated for CO in the JQ tunnel and for temporal

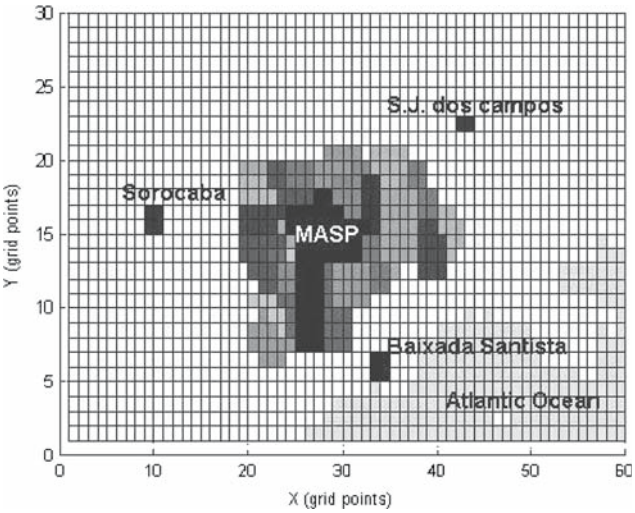

Fig. 3 Spatial distribution of CO, RHC, NO_x and SO_2 motor vehicles emissions in the MASP, Sorocaba, São José do Campos (S.J. dos Campos) and Baixada Santista. The scale grey is proportional to the emission amount. The largest emission are 47.9 kg min^{-1} for CO, 10.4 kg min^{-1} for RHC, 9.7 kg min^{-1} for NOx and 1.0 kg min^{-1} for SO2

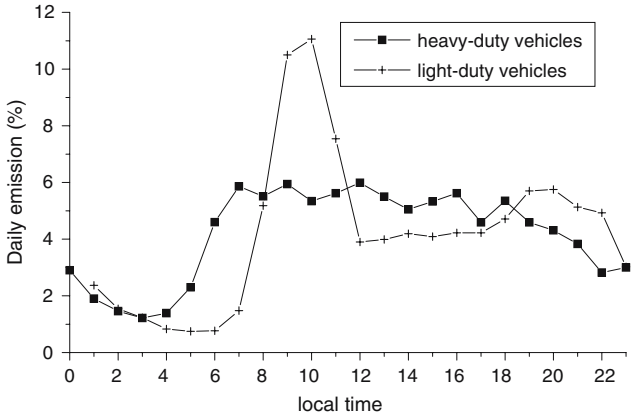

Fig. 4 Mobile emission hourly distribution, in each cell CIT model, for light-duty vehicles and heavy-duty vehicles in % (The values of daily emission were divided by factor 0.01)

distribution of HDVs (a relatively continuous emission from 0600 to 1800 LT), it used the EFs estimated for NO_x in the MM tunnel.

The species used to represent the organic mobile vehicles emissions were: Acetone; alkane group 1; alkane group 2; alkane group 3; aromatics 1; aromatics 2; benzaldehyde; 1,3-butadiene; benzene; acetaldehyde; ethanol; formaldehyde; isoprene; methyl ethyl ketone; methanol; olephines 1; olephines 2 and aldehydes. The species in SAPRC-99 are grouped by reactivity of the compounds. These compounds were scaled proportionally according to ambient measurements made by Colón et al. [47] and by Martins et al. [45] On the other hand, for species organic point source emissions

Table 7 Adjusted vehicles emissions scaling factors for the base case for 13–16 March 2000 in the Sao Paulo metropolitan area

Species	March 13	March 14	March 15
NO—Nitrogen monoxide	0.62	0.45	0.94
CO—Carbon monoxide	0.73	1.35	1.27
SO_2—Sulfur dioxide	1.0	1.0	1.0
ACET—Acetone	0.8	1.4	1.0
ALK1—Alkanes 1	0.8	1.4	1.0
ALK2—Alkanes 2	0.8	1.4	1.0
ALK3—Alkanes 3	0.8	1.4	1.0
ARO1—Aromatics 1	0.8	1.4	1.0
ARO2—Aromatics 2	0.8	1.4	1.0
BALD—Benzaldehyde	0.8	1.4	1.0
BUTD—Butadiene	0.8	1.4	1.0
C6H6—Benzene	0.8	1.4	1.0
CCHO—Acetaldehyde	0.8	1.4	1.0
ETOH—Ethanol	0.8	1.4	1.0
HCHO—Formaldehyde	0.8	1.4	1.0
ISOP—Isoprene	0.8	1.4	1.0
MEK—methyl ethyl ketone	0.8	1.4	1.0
MEOH—methanol	0.8	1.4	1.0
OLE1—Olefines 1	0.8	1.4	1.0
OLE2—Olefines 2	0.8	1.4	1.0
RCHO—Aldehydes	0.8	1.4	1.0

were: alkane group 1; alkane group 2; aromatics 1; aromatics 2; ethanol; olephines 1 and olephines 2 [48].

The motor vehicle emissions inventories data provided by CETESB [33] were adjusted to a factor based on top-down analysis (starting with ambient concentration), in this study, we performed RHC/CO and NO_x/CO mass ratios derived from ambient measurement. These scaling factors are presented in Table 7. Ambient concentration data provide a useful independent check on mobile source emission inventories. There have been several studies of mobile source emission estimates based on ambient pollutant ratios [3,11,32,49]. Andrade et al. [32] and Vivanco and Andrade [11] found that the ration RHC/NO_x in the CETESB inventory is significantly low when compared to observed ration.

2.5 Initial and boundary conditions

Initial pollutant concentrations fields were constructed according to Goodin et al. [34] using hourly average of carbon monoxide, ozone, sulfur dioxide, nitric oxide, nitrogen dioxide and Reactive hydrocarbons (RHC) air quality data collected at monitoring stations in the MASP, were interpolated to the computational grid. Table 8 shows the initial conditions values used for CIT simulations. These values are used only at the start of the first day of simulations (13 March 2000). At the end of the first day of simulations, the concentrations of all species are saved and these values are used to start the second day of simulation (14 March 2000). At the end of these second day, also the concentrations of all species are saved and these values are used to start the third day of CIT simulations (15 March 2000). The first day was devoted to a spin-up period in order to minimize the influence of assumed initial conditions [29,50]. Inflow

Table 8 Initial conditions (ppbv) used for the simulation of air quality for 13–16 March 2000 in the Sao Paulo metropolitan area

Vertical layer in model[a]					
Species	Surface	Level 2	Level 3	Level 4	Level 5
CO	aq[b]	Aq	0.0	0.0	0.0
SO_2	aq	Aq	0.0	0.0	0.0
NO_2	aq	Aq	0.0	0.0	0.0
NO	aq	Aq	0.0	0.0	0.0
O_3	aq	pd[c]	pd	pd	Pd
RHC[d]	aq	Aq	100.0	100.0	200.0

[a] The CIT model has five vertical layers with elevations above ground level of: (1) 0–73 m; (2)74–294; (3) 295–588; (4) 599–1281; (5) 1282–2100

[b] An entry of aq means that the value is from an interpolated air quality field baesd on actual measurements made on 13–15 March 2000

[c] An entry of pd means that the values is from an interpolated air quality field based on actual measurements from the previous day's mid-afternnon surface level values

[d] RHC expressed in units of ppbC

Table 9 Inflow boundary conditions (ppbv) used for the simulation of air quality for 13–15 March 2000 in the Sao Paulo metropolitan area

Vertical layer in CIT model[a]						
Species	Boundary	Surface	Level 2	Level 3	Level 4	Level 5
CO	N,E,S,W	200.0	200.0	200.0	200.0	200.0
SO_2	North, West	1.0	1.0	1.0	1.0	1.0
SO_2	East, South	2.0	2.0	2.0	2.0	2.0
NO_2	N,E,S,W	1.0	1.0	1.0	1.0	1.0
NO	N,E	1.0	1.0	1.0	1.0	1.0
NO	S,W	2.0	2.0	2.0	2.0	2.0
O_3	N,W	5.0	5.0	5.0	5.0	5.0
O_3	E, S	4.0	4.0	4.0	4.0	4.0
RHC[b]	N,E,S,W	100.0	100.0	100.0	100.0	100.0

[a] The CIT model has five vertical layers with elevations above ground level of: (1) 0–73 m; (2)74–294; (3) 295–588; (4) 599–1281; (5) 1282–2100

[b] RHC expressed in units of ppbC

boundary conditions are set based on pollutant concentrations measurements made near the edges of the MASP modeling region [51] (Table 9).

2.6 Description of the RAMS 4.3 application

The RAMS 4.3 application [6] utilizes an Arakawa C-grid on a rotated polar stereographic projection and employs a terrain-following coordinate system that determines the vertical coordinate. The RAMS 4.3 simulations were performed for the period of March 12–16, 2000 using two nested grids with horizontal grid resolutions of 20 and 5 km, respectively [52,53]. The outer domain encompassed most of the state of São Paulo, whereas the inner domain encompassed only the MASP (see Fig. 5). The simulated horizontal wind in the second grid is shown in Fig. 6. Thirty-two vertical layers with vertical grid spacing ranging from 60 to 1000 m and a vertical grid stretch ratio of 1.2 were used in the simulations. The numbers of grid cells in the east–west

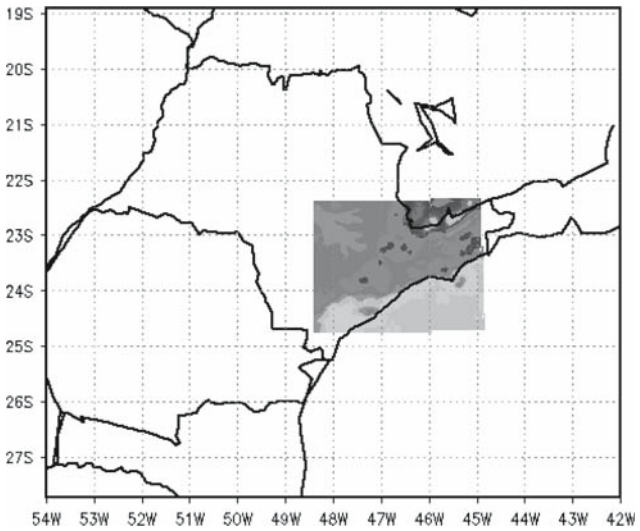

Fig. 5 RAMS simulation domain. The coarse and fine (shaded) grid intervals are 20 and 5 km, respectively

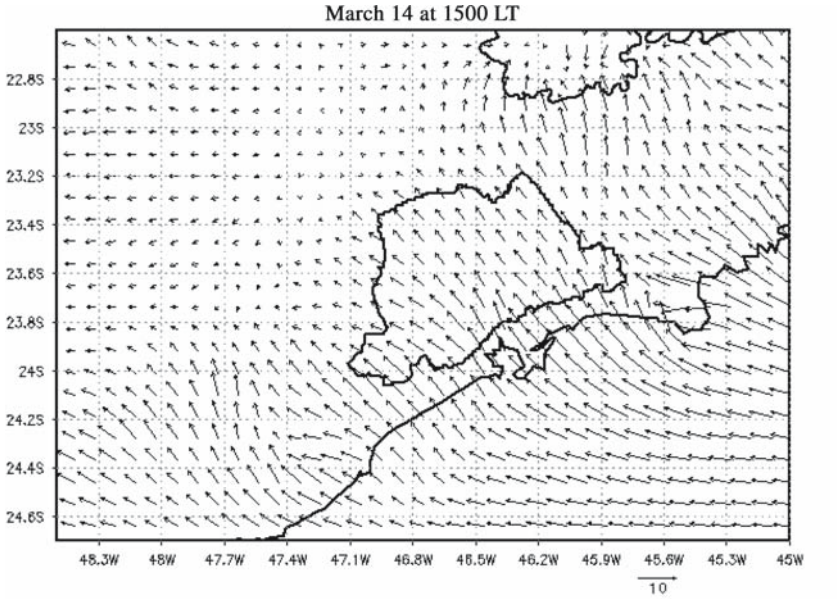

Fig. 6 Predicted horizontal wind field obtained from the RAMS version 4.3 at 33 m on March 14, 2000 at 1500 local time (LT), used as input to CIT model

and north–south directions were 82 × 46 and 74 × 54, respectively, at the 20 and 5 km grid resolutions. Four-dimensional data assimilation was employed using input fields from global analysis fields, obtained from the Brazilian Center for weather forecasting and climate studies reanalysis data at 1.875° horizontal resolution and 6-h time intervals [54]. A scheme which employs prognostic turbulent kinetic energy approach [55] was utilized to parameterize the vertical diffusion, while the parameterization of the horizontal diffusion coefficients was performed based on the K-theory as used by Smagorinski [56]. A convective parameterization scheme was initiated. The radiation parameterization used the Harrington scheme [57], and bulk microphysics parameterization was activated. The study also utilized a soil/vegetation model.

2.7 Observed synoptic features for the episode of March 13–16, 2000.

On March 5, 2000, a cold front arrived in the State of Rio Grande Sul (in the south of Brazil). This cold front passed by the São Paulo coastline on March 8. The same cold front reached the state of Bahia (in the northeast of Brazil) on March 11. This cold front remained stationary until March 15, exiting the country on March 16 [58]. The observed synoptic features of the ozone episode during March 13–16, 2000 can be classified as a post-frontal condition, based of large-scale systems namely the relative positions, the nature and types of the anticyclone or cold front [59]. Thus, in the CIT model was considered all post-frontal status, with prevailing winds from the southeast bringing air into the MASP from over the Atlantic Ocean.

3 Results and discussion

For the validation of the model, the ozone, NO_x, RHC, and CO concentrations from model's first vertical level for the base case were compared with surface observations. The times series of simulated and observed concentrations are presented in Fig. 7. In this figure, vertical bars indicate the maximum and minimum values of the pollutant concentrations measured at different air quality stations: (i) for ozone six stations that are indicated in Fig. 2, (ii) for NO_x three stations that are IBIR, PQDP and SCSU, (iii) for CO eight stations that are IBIR, PQDP, OSAS, SCSU, CCES, LAPA, SACT and SAMO. In this figure, the model reproduces the diurnal pattern of observed ozone concentrations, but over predicts observed peak ozone concentrations on March 13 and 14. Still, the nocturnal ozone concentrations were zero, maybe resulting from an inappropriate represent of the nocturnal boundary layer process. Peak observed ozone concentration on March 14 occurred at 1400 LT with average 65 ppbv, while the peak observed ozone concentration on March 15 occurred at 16 LT with average 45 ppbv. Also, simulated primary pollutant concentrations for the MASP are in agreement with the average observed values except for some discrepancies at daytime on March 15, 2000 that are: (i) simulations under predicted CO and RHC concentrations, (ii) predicted NO_x concentrations were higher than observed concentrations. As pointed out by Chandrasekar et al. [60], observations are primarily point measurements whereas the model predictions are grid values. Also, the difference between heights where the measurements were made could be the reason for some disagreement. Average CO concentrations measured during the 13–15 March episode were in the 0–2 ppm range. As shown in Fig. 7, both predicted and observed CO concentrations are highest during the morning peak traffic period in the MASP.

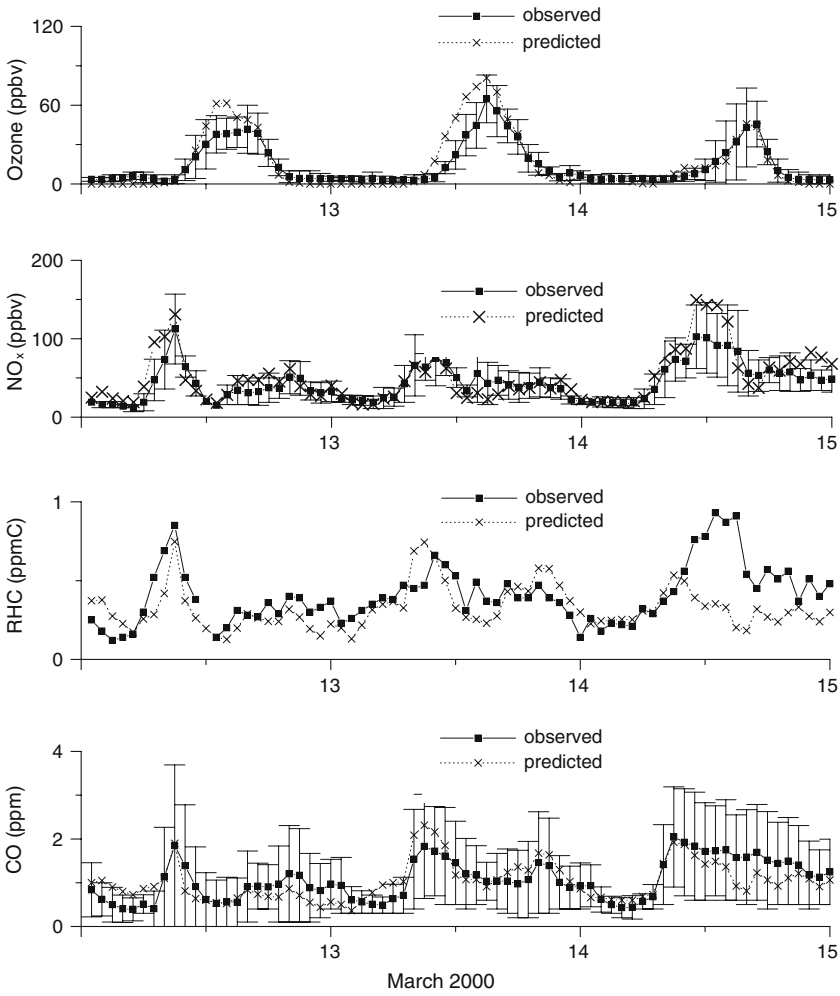

Fig. 7 Time series plots of measurements of various species from 13 to 15 March 2000 in the MASP, on comparison with base case model result. Vertical bars indicate the standard deviation of the measured pollutants concentrations

To evaluate the CIT airshed model against the measured concentrations of air quality species, a model performance evaluation was calculated to complement the qualitative graphical time series analysis (Fig. 7). A variety of statistical measures have been developed to quantitatively specify air quality model performance [61,62], such as: (i) mean error (BIAS), (ii) mean normalized Bias, (iii) mean Gross Error (Gross error), and (iv) mean normalized Gross Error. The bias is computed as the mean residual, where the residual is the predicted minus observed concentration. Therefore, negative bias implies under prediction of observation by the CIT model. Gross error is computed in the same manner as bias, except that the absolute values of the residual are used, so gross error is always positive. Normalized bias and gross error are computed by dividing each residual by the corresponding observed concentration

Table 10 Comparison of species observations from air quality stations located in the Sao Paulo metropolitan area

Statistical measure[a]	14 March	15 March	Total
Ozone			
Bias (ppbv)	9.6	0.91	5.3
Normalized bias (%)	15.2	2.7	9.0
Gross error (ppbv)	11.9	2.1	7.0
Normalized gross error (%)	33.2	5.3	19.3
CO			
Bias (ppmv)	0.13	−0.25	−0.1
Normalized bias (%)	12.1	−0.16	6.0
Gross error (ppmv)	0.25	0.27	0.3
Normalized gross error (%)	24.5	19.1	21.8
NO_x			
Bias (ppbv)	−3.6	12.7	4.6
Normalized bias (%)	5.8	20.1	13.0
Gross error (ppbv)	7.2	16.9	12.1
Normalized gross error (%)	18.8	26.8	22.8
RHC			
Bias (ppmC)	−0.003	−0.15	−0.1
Normalized bias (%)	2.2	−18.8	−8.3
Gross error (ppmC)	0.1	0.19	0.1
Normalized gross error	30.2	32.4	31.3

before averaging. Whenever the observed ozone, CO, NO_x concentrations are below the specified cutoff levels of 30 ppbv, 0.5 ppm, and 20 ppb, respectively, the observed and predicted concentrations for that hour and location are not used in computing the statistical analysis [63,64]. The US Environmental Protection Agency (US EPA) [64] guideline states that the performance evaluation results would be acceptable when normalized bias, and gross error statistics fall within the range of (±)5–15%, and 30–35%, respectively. Table 10 shows the performance evaluation results of the present modeling on a daily basis in terms of the statistical measures described above. First, for the whole period, the normalized bias of 9.0, 6.0, 13.0, and −8.3 for ozone, CO, NO_x, and RHC, respectively, which indicate a good performance of CIT model. Normalized gross error indicate a better performance for RHC, while the slightly good performance for ozone, CO, and NO_x. However statistical analysis varies greatly from day to day and for each pollutant.

Figure 8a shows the spatial distributions of predicted ozone concentration (in ppbv), obtained using the base case scenario for March 14 at 1400 LT. Predicted ozone concentrations are low (20–40 ppbv) near the cost (located at SE of São Paulo City), east edge, and central portion north of the model domain. One area (ozone plume) of high ozone concentration (approximately 160 ppbv) is shown. This area is located in the west portion of the MASP. It seems that RHC and NO_x from metropolitan traffic and industrial emissions not only could cause high ozone concentration in the urban area, but also can be transported downwind towards an area unfavorable for pollutant dispersion, thus affecting an area that has few emissions of RHC and NO_x such as SORO [61,65]. In Fig. 8b, the spatial distribution of predicted ozone concentrations for March 15 at 1500 LT is shown. The average predicted ozone concentration in the area of six air quality stations for ozone was about 45 ppbv (Fig. 7), in agreement with the spatial pattern of those average observed ozone concentration

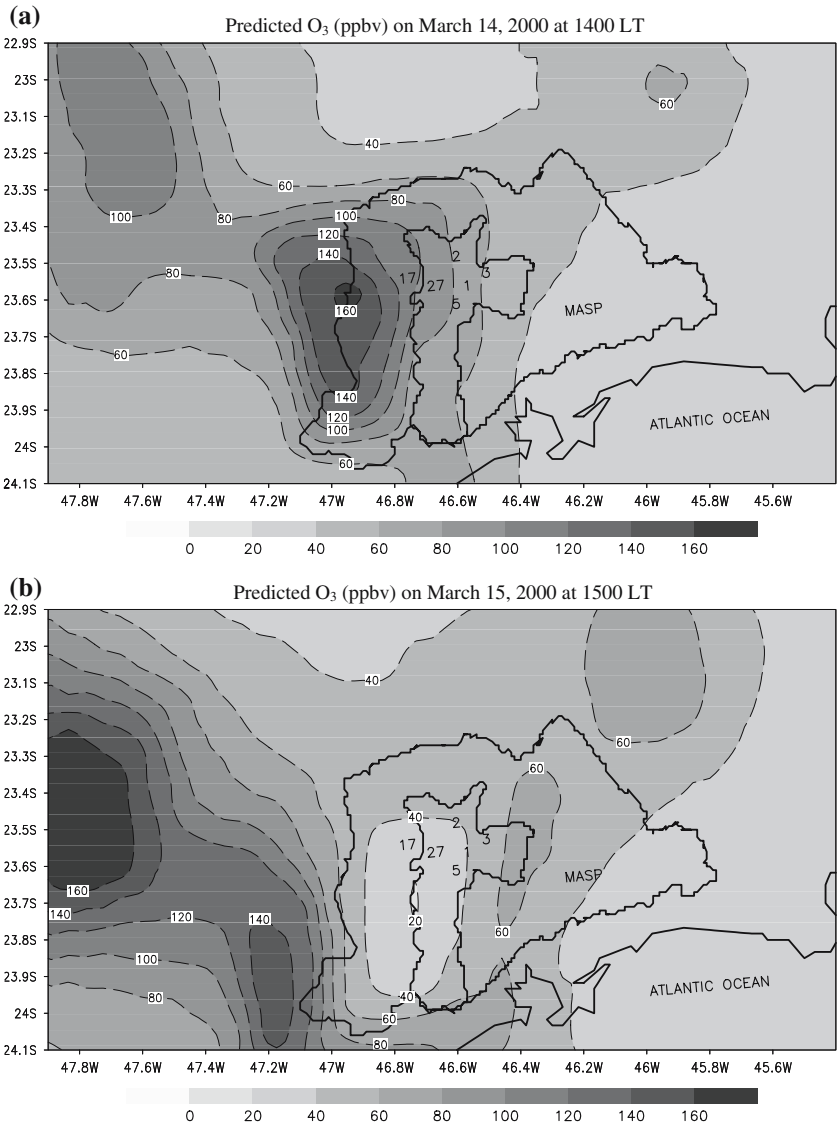

Fig. 8 Spatial distribution of predicted ozone concentrations (in ppbv) using the year 2000 CETESB emission inventory scenario, base case scenario: (**a**) March 14 at 1400 LT, (**b**) March 15 at 1500 LT. The numbers indicate the air quality stations showed in Table 6

of 43 ppbv. Peak ozone concentration, highest ozone concentration (approximately 160 ppbv), was located in the northwest edge of the MASP. It is likely that, on this day, ozone, as well as its precursors, were transported by prevailing southeasterly winds to this area, thereby contributing to the high ozone concentrations. Figure 9 shows the spatial distribution of predicted NO_x concentrations (in ppbv) in the base case scenario. The NO_x spatial distribution in the domain reflects mainly the NO_x emission pattern in the MASP, the most important source of NO_x is heavy-duty diesel

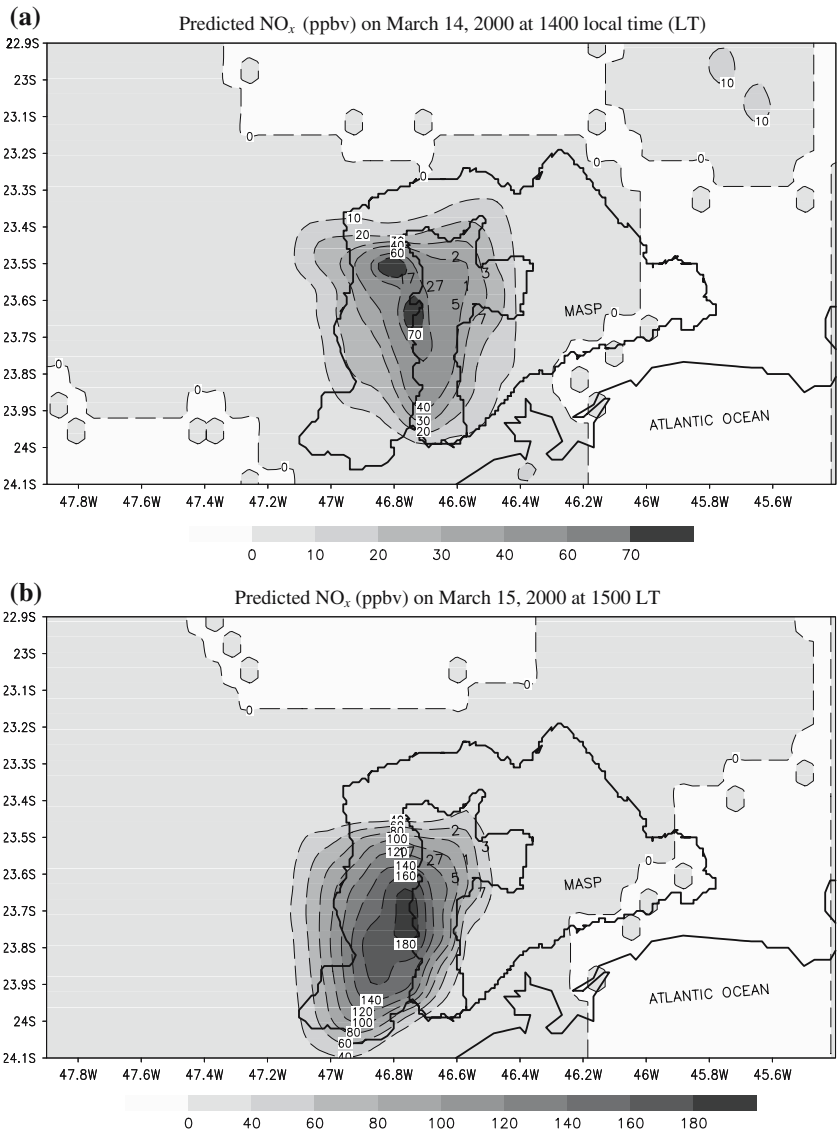

Fig. 9 Spatial distribution of predicted nitrogen oxide NO_X concentrations (in ppbv) at the first level, base case scenario: (**a**) on March 14, 2000 at 1400 LT and (**b**) on March 15, 2000 at 1500 LT

vehicles. At the location of the ozone plume, on March 14 at 1400 LT, the NO_x is low (approximately 20 ppbv), while at outside of the MASP, on March 15 at 1500 LT, the predicted NO_x concentration are nill.

Figure 10 shows the comparisons among the different scenarios, including the base case scenario, regarding average ozone concentration at the six air quality monitoring station in the MASP, those stations are indicated in Fig. 2. Simulated ozone concentrations were higher when emissions inventory, scenario 2 was used. The results obtained in the CIT modeling showed that, without the implementation of the PROCONVE,

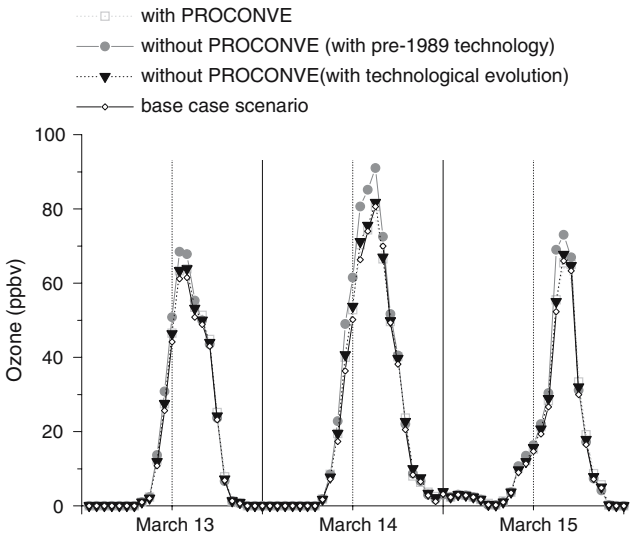

Fig. 10 Comparison among the different scenarios and base case average ozone concentrations in the MASP from March 13 to 15, 2000

ozone concentrations would be higher than those obtained in the scenario including PROCONVE implementation. The PROCONVE implementation reduced the emission of ozone precursors and consequently reduced ozone levels when compared with a scenario without PROCONVE. However, the reduction of ozone levels was more pronounced when compared with scenario without PROCONVE and pre-1989 technology. In addition, the reduction was higher for CO levels. The ozone concentrations in general do not follow correspondingly to reduction of the precursors; because the ozone formation is dependent of VOCs-NO_x rations, and for ozone control it is recommended to know this relation in the area for establishing strategies of ozone control.

4 Summary and conclusions

Herein, we have presented modeling results regarding the impact that implementing a national motor vehicle pollution control program has on ozone concentrations in Brazil. To that end, the CIT three-dimensional chemistry model [37] was used to analyze the high surface ozone episode occurring on March 13–15, 2000 in the MASP.

Based on statistical metrics and graphical time series analysis, the ozone, reactive hydrocarbons, oxides of nitrogen and carbon monoxide concentrations simulated for the base case scenario were in agreement with observations. However, the ozone concentrations simulated for the nocturnal period were nil, probably resulting from an inaccurate representation of the nocturnal boundary layer process.

High levels of ozone have been simulated, using the CIT model, in the MASP and downwind area, indicating that RHC and NO_x emissions from motor vehicles and industrial not only can originate elevated ozone concentration in the MASP area

(urban area), but also can be transported downwind toward affecting an area with low emission of RHC and NO_x.

The implementation of the PROCONVE in the MASP resulted in improved air quality, not only in terms of primary pollutants but also in terms of ozone levels, however much less pronounced.

Although the implementation of an emissions control program requires considerable expenditure, the benefits in improved air quality can outweigh the costs if we consider that this is directly related to an improvement in public health.

Acknowledgements This study was supported by the *Fundação de Amparo à Pesquisa do Estado de São Paulo* (FAPESP, Foundation for the support of research in the State of São Paulo; project No. 96\0143–4 and project No. 02/09060). The authors wish to express their gratitude to Mr. Jefferson Boyles for reviewing the manuscript. Helpful comments of anonymous referees are appreciated. We also wish to thank Robert Harley of University of California at Berkeley, provided helpful discussion.

References

1. Sillman S (1999) The relation between ozone, NO_x and hydrocarbons in urban and polluted rural environments. Atmos Environ 33:1821–1845
2. Held T, Ying Q, Kaduwela A, Kleeman M (2004) Modeling particulate matter in the San Joaquin Valley with a source-oriented externally mixed three-dimensional photochemical grid model. Atmos Environ 38:3689–3711
3. Mellios G, Aalst VR, Samaras Z (2006) Validation of road traffic urban emission inventories by means of concentration data measured at aair quality monitoring station in Europe. Atmos Environ 40:7362–7377
4. La Rovere EL (2002) Avaliação do PROCONVE programa de Controle da Poluição do Ar por Veículos Automotores. Laboratório Interdisciplinar de Meio Ambiente- COPPE/UFRJ. Universidade Federal de Rio Janeiro, Rio de Janeiro, Brasil, pp 187
5. McRae GJ, Goodin WR, Seinfeld JH (1982a) Development of second-generation mathematical model for urban air pollution- I. Model Formulation. Atmos Environ 16:679–696
6. Cotton WR, Pielke RA, Walko S, Liston RL, Tremback GE, Jiang HC, McAnelly RL, Harrington JY, Nicholls ME, Carrio GG, McFadden JP (RAMS 2001: 2003) Current status and future directions. Meteorol Atmos Phys 82:5–29
7. Pielke RA, Cotton WR, Walko RL, Tremback CJ, Lyons WA, Grasso LD, Nicholls ME, Moran MD, Wesley DA, Lee TJ, Copeland JH (1992) A Comprehensive meteorological modeling system – RAMS. Meteorol Atmos Phys 49(1–4):69–91
8. Harley RA, Russell AG, McRae GJ, Cass GR, Seinfeld JH (1993) Photochemical modeling of the Southern California Air Quality Study. Envir Sci Technol 27:378–388
9. Burian SJ, Streit GE, McPherson TN, Brown MJ, Turin HJ (2001) Modeling the atmospheric deposition and stormwater washoff of nitrogen compounds. Env Model S 16:467–479
10. Sánchez-Ccoyllo OR, Ynoue YR, Martins DL, Andrade FM (2006) Impacts of ozone precursor limitation and meteorological variables on ozone concentration in Sao Paulo, Brazil. Atmos Environ 40:S552-S562
11. Vivanco GM, Andrade FM (2006) Validation of the emission inventory in the São Paulo Metropolitan área of Brazil, base don ambient concentrations ratios of CO, NMOG, and NO_x and on a photochemical model. Atmos Environ 40:1189–1198
12. Ulke AG, Andrade MF (2001) Modeling urban air pollution in Sao Paulo, Brazil: sensitivity of model predicted concentrations to different turbulence parameterizations. Atmos Environ 35:1747–1763
13. CETESB (2004) Relátorio de Qualidade do Ar no Estado de São Paulo-2003. Série Relatórios ISSN-0103–4103. Companhia de Tecnologia de Saneamento Ambiental, São Paulo, Brazil. http://www.cetesb.sp.gov.br
14. Silva Dias MAF, Machado AJ (1997) The role of local circulations in summertime convective development and nocturnal fog in São Paulo, Brazil. Boundary-Layer Met 82:135–157
15. Kuebler J, Giovannoni J, Russel AG (1996) Eulerian modeling of photochemical pollutants over the Swiss plateau and control strategy analysis. Atmos Environ 30:951–966

16. McRae JG, Tilden WJ, Seinfeld HJ (1982b) Global sensitivity analysis-A computiational implementation of the Fourier Amplitude Sensitivity Test (FAST). Comp Chem Eng 6:15–25
17. Falls HA, McRae JG, Seinfeld HJ (1979) Sensitivity and uncertainty of reaction mechanisms for photochemical air pollution. Int J chem Kinet XI:1137–1162
18. Koda M, Dogru AH, Seinfeld JH (1979) Sensitivity analysis of partial differential equations with applications to reaction and diffusiom processes. J Computat Phys 30(2):259–283
19. Seefeld S, Stockwell RW (1999) First-order sensitivity analysis of models with time-depent parameters: an application to PAN and ozone. Atmos Environ 33:2941–2953
20. Daescu ND, Sandu A, Carmichael RG (2003) Direct and adjoint sensitivity analysis of chemical kinetic systems with Kinetic Pre-Processor: II- Numerical validations and applications. Atmos Environ 37:5097–5114
21. Kioutsioukis I, Tarantola S, Saltelli A, Gatelli D (2004) Uncertainty and global sensitivity analysis of road transport emission estimates. Atmos Environ 38:6609–6620
22. Mulholland M, Seinfeld JH (1995) Inverse air pollution modeling of urban-scale carbon monoxide emissions. Atmos Environ 29:497–516
23. Nguyen K, Dabdub D (2003) Development and analysis of a non-splitting solution for three dimensional air quality models. Atmos Environ 37:3741–3748
24. Carter WPL (2000a) Implementation of the SAPRC-99 chemical mechanism into the models-3 framework "Report to the United States environmental protection agency". January, 29, http://pah.cert.ucr.edu/∼carter/reactdat.htm
25. Carter WPL (2000b) Documentation of the SAPRC-99 chemical mechanism for VOC reactivity assessment. Final report to california air resources board contract No. 92–329, and (in part) 95–308, May 8, http://pah.cert.ucr.edu/∼carter/reactdat.htm
26. Carter WPL (1990) A detailed mechanism for the gas-phase atmospheric reactions of organic compounds. Atmos Environ 24A:481–518
27. Carter WPL (1994) Development of ozone reactivity scales for volatile organic compounds. J Air Waste Manage Assoc 44:881–899
28. Carter WPL, Atkinson R (1996) Development and evaluation of a detailed mechanism for the atmospheric reactions of isoprene and NOx. Int J Chem Kinet 28:497–530
29. Kim JY, Ghim YS (2002) Effects of the density of meteorological observations on the diagnostic wind fields and the performance of photochemical modeling in the greater Seoul area. Atmos Environ 36:201–212
30. Liston GE, Pielke RA (2001) A climate version of the regional atmospheric modeling system. Theor Appl Climatol 68:155–173
31. Gesch DB, Verdin KL, Greenlee SK (1999) New land surface digital elevation model covers the Earth. EOS Trans Amer Goeophys Un 80(6):69–70
32. Andrade MF, Ynoue RY, Harley R, Miguel AH (2004) Air-quality model simulating photochemical formation of pollutants: the São Paulo metropolitan area, Brazil. Int J Environ Pollut 22(4):460–475
33. CETESB (2001) Relátorio de Qualidade do Ar no Estado de São Paulo-2000. Série Relatórios ISSN-0103–4103. Companhia de Tecnologia de Saneamento Ambiental, São Paulo, Brazil. http://www.cetesb.sp.gov.br
34. Goodin WR, McRae GJ, Seinfeld JH (1979) A comparison of interpolation methods for sparse data: application to wind and concentration fields. J Appl Meteorol 18:761–771
35. Nair KN, Freitas ED, Sánchez-Ccoyllo OR, Silva Dias MAF, Silva Dias PL, Andrade MF, Massambani O (2004) Dynamics of urban boundary layer over São Paulo associated with mesoscale processes. Meteorol Atmos Phys 86(1–2):87–98
36. Barnes SL (1973) Mesoscale objective map analysis using weighted time-series observations. NOAA technical memorandum ERL NSSL-62, National Oceanic and Atmospheric Administration, Norman
37. McRae GJ (1981) Mathematical modeling of photochemical air pollution, Ph.D. Thesis, California Institute of Technology, Pasadena, California
38. McRae GJ, Russell AG, Harley RA (1992) CIT photochemical airshed model- Systems Manual, Carnegie Mellon University, Pittsburgh, Pennsylvania and California Institute of Technology, Pasadena, California
39. Peterson JT (1976) Calculated actinic fluxes (290–700 nm) for air pollution photochemistry applications US environmental protection agency: reasearch triangle parck, NC, EPA-600/4–76–025 pp 63

40. Lyons WA, Tremback CJ, Pielke RA (1995) Applications of the regional atmospheric modeling system (RAMS) to provide input to photochemical grid models for the Lake Michigan ozone study (LMOS). J Appl Met 34:1762–1786
41. Pielke RA, Uliaz M (1998) Use of meteorological models as input to regional and mesoscale air quality models-limitations and strengths. Atmos Environ 32:1455–1466
42. Russell GA, Winner AD, Harley AR, McCue FK, Cass RG (1993) Mathematical modeling and control of the dry deposition flux of nitrogen-containing air pollutants. Environ Sci Technol 27(13):2772–2782
43. Alonso DC, Martins BRHM, Romano J, Godinho R (1997) São Paulo aerosol characterization study. J Air Waste Manage Assoc 47:1297–1300
44. DETRAN (2001) http://www.detran.sp.gov.br (accessed in September 2004)
45. Martins LD, Andrade MF, Freitas ED, Pretto A, Gatti LV, Albuquerque EL, Tomaz E, Guardani ML, Martins MHRB, Junior OMA (2006) Emission factors for gas-powered vehicles traveling through road tunnels in São Paulo city, Brazil. Environ Sci Technol 40:6722–6729
46. Sánchez-Ccoyllo OR, Ynoue YR, Martins DL, Astolfo, Miranda MR, Freitas DE, Borges SA, Fornaro A, Moreira A, Maria F, Andrade FM (2006) Vehicular particulate matter emissions from road tunnels in Sao Paulo city, Brazil. Transportation. Res Part D: Transport Environ (Submitted)
47. Colón M, Pleil JD, Hartlage TA, Guardani ML, Martins MH (2001) Survey of volatile organic compounds associated with automotive emissions in the urban airshed of São Paulo, Brazil. Atmos Environ 35:4017–4031
48. Sexton K, Westburg HH (1983) Photochemical ozone formation from Petroleum Refinery emissions. Atmos Environ 17:467–475
49. Harley AR, Sawyer FR, Milford BJ (1997) Updated photochemical modeling for California's south cost air caisn: comparison of chemical mechanisms and motor vehicle emission inventories. Environ Sci Technol 31:2829–2839
50. Baertsch-Ritter N, Prevot AH, Dommen J, Andreani-Aksoyoglu S, Keller J (2003) Model study with UAM-V in the Milan area (I) during PIPAPO: simulations with changed emissions compared to ground and airborne measurements. Atmos Environ 37:4133–4147
51. Winner DA, Cass GR, Harley RA (1995) Effect of alternative boundary conditions on predicted ozone control strategy performance: A case study in the los Angeles Area. Atmos Environ 29:3451–3464
52. Sanchez-Ccoyllo OR, Silva Dias PL, Andrade MF, Freitas SR (2005) Determination of O_3, CO and PM_{10} transport in the metropolitan area of São Paulo, Brazil through synoptic scale analysis of back trajectories. Meteorol Atmos Phys 92:83–93
53. Freitas RS, Longo MK, Silva Dias MAF, Silva Dias PL, Chatfield R, Prins E, Artaxo P, Grell GA, Recuero SF (2005) Monitoring the transport of biomass burning emissions in South America. Environ Fluid Mech 5:135–167
54. Cavalcanti IFA, Marengo JA, Satyamurty P, Nobre CA, Trosnikov I, Bonatti JP, Manzi AO, Tarasova T, Pezzi LP, D'Almeida C, Sampaio G, Castro CC, Sanches MB, Camargo L (2002) Global climatological features in a simulation using the CPTEC-COLA AGCM. J Climate 15(21):2965–2988
55. Mellor GL, Yamada T (1982) Development of a turbulence closure model for geophysical fluid problems. Rev Geophys Space Phys 20(4):851–875
56. Smagorinski J (1963) General circulation experiments with the primitive equations. Part I, the basic experiment. Mon Wea Rev 91:99–164
57. Harrington JY (1997) The effects of radiative and microphysical processes on simulated warm and transition season Artic stratus. Ph.D. dissertation. Atmos Sci Paper No. 637, Department of Atmospheric Science, Colorado State University, Fort Collins, CO, 80523, 1–289
58. Climanalise (2000) Boletim de Monitoramento e Análise Climática, 15(3) March 2000, http:/www.cptec.inpe.br (accessed in April 2004)
59. Sánchez-Ccoyllo OR, Andrade MF (2002) The influence of meteorological conditions on the behaviour of pollutants concentrations in São Paulo. Environ Pollut 116:257–263
60. Chandrasekar A, Philbrick CR, Doddridge B, Clark R, Georgopoulos P (2003) A comparison study of RAMS simulations with aircraft, wind profiler, lidar, tethered balloon and RASS data over Philadelphia during a 1999 summer episode. Atmos Environ 37:4973–4984
61. Lee RF, Irwin JS (1995) Methodology for a comparative evaluation of 2 air-quality models. Int J Environ Pollut 5(4–6):723–733

62. Seigneur C, Pun B, Pai P, Louis JF, Solomon P, Emery C, Morris R, Zaniser M, Worsnop D, Koutrakis P, White W, Tombach I (2000) Guidance for the performance evaluation of thee-dimensional air quality modeling systems for particulate matter and visibility. J Air Waste Manage Assoc 50:588–599
63. US EPA (US Environmental Protection Agency) (1995) Guideline for regulatory application of the urban airshed model. Research Triangle Park, Noth Carolina, 27711
64. US EPA (US Environmental Protection Agency) (2005) Guidance on the use of models and other analyses in attainment demonstrations for the 8-hour ozone NAAQS, EPA-454/R-05–002, http://www.epa.gov/scram001/ (accessed in October 2006)
65. Cheng LW (2000) A vertical profile of ozone concentration in the atmospheric boundary layer over central Taiwan. Meteorol Atmos Phys 75:251–258